Publishing Excellence Inspiring Progress
ARISTON PUBLICATIONS
EEA Energy & Environment Advances
ISSN: xxxx-xxxx https://aristonpubs.com/energy-environment-advances https://doi.org/10.69626/eea.2024.0206

RESEARCH ARTICLE

Enhanced Adsorption Characteristics of Methylene Blue Dye using CNT–Functionalized Moringa Leaf Powder

Anu Malhotra [1, 2], Suchitra Manjhu [3], Harish Kumar Meena [3], Karishma Jain [4], Sonia Srivastava [2], Anju Lavania [2], S.K. Jain [4], Rama S Lokhande [1], Balram Tripathi [2, *]

ABSTRACT: This study investigates the adsorption potential of methylene blue (MB) dye using a novel bio-composite prepared by intercalating carbon nanotubes (CNTs) with Moringa oleifera leaf powder (MOLP). Adsorption capacity optimization was performed under varying experimental conditions, including pH (4–9), initial MB concentration (0.05–1 ppm), adsorbent dosage, temperature (20–50°C), and contact time (0–60 minutes). The biosorbent's surface properties and functional groups were characterized through Scanning Electron Microscopy (SEM) and Fourier Transform Infrared (FT-IR) spectroscopy, revealing the synergistic role of CNT intercalation in enhancing adsorption efficiency. SEM analysis confirmed a heterogeneous, porous morphology of MOLP, ideal for dye entrapment. FT-IR spectra indicated the presence of carboxylic, carbonyl, and phenolic groups, which significantly contributed to the binding of MB dye molecules through hydrogen bonding and electrostatic interactions. The results demonstrate that functionalized MOLP exhibits superior adsorption performance compared to pristine MOLP, owing to the remarkable surface area and tunable chemistry of CNTs. This study highlights the potential of CNT-MOLP as a cost-effective, sustainable adsorbent for wastewater treatment, offering an efficient alternative to conventional methods for dye removal.

Keywords: Carbon nanotubes, Moringa oleifera, Dye adsorption, Wastewater treatment, Adsorption mechanism

Received: 15 June 2024; Revised: 19 July 2024; Accepted: 23 August 2024; Published Online: 15 September 2024

1. INTRODUCTION

Dyes are widely used in many industries, including textile, paper, plastic, leather, and rubber manufacturing, due to their ability to impart vibrant colors to products. However, most of these dyes are synthetic and pose significant environmental challenges when discharged into wastewater without proper treatment. The synthetic dyes used in these industries, especially quinone and azo compounds, are non-biodegradable and persistent in the environment, leading to severe ecological and health concerns. Globally, the annual production of organic dye compounds exceeds 700,000 tons, primarily due to their widespread applications in cosmetics, food, pharmaceuticals, textiles, and leather industries [1–3]. The untreated discharge of these dyes into water bodies creates significant environmental burdens as they resist degradation by natural, chemical, or photolytic processes, thereby accumulating in the ecosystem.

The harmful effects of synthetic dyes are not limited to environmental contamination; they also have toxicological impacts on flora, fauna, and humans. Many dyes and their degradation intermediates are known to be carcinogenic, teratogenic, and mutagenic [4]. Among these dyes, methylene blue (MB) is extensively used in the textile industry. It is vital to remove MB and similar dyes from industrial effluents to mitigate their harmful effects on the environment. Conventional water treatment methods, while

[1] Department of Chemistry, Jaipur National University, Jaipur-302018, India
[2] Department of Physics, S S Jain Subodh PG College, Jaipur-302004, India
[3] Department of Physics, University of Rajasthan, Jaipur-302004, India
[4] Department of Physics, Manipal University Jaipur, Jaipur-302017, India

* Author to whom correspondence should be addressed: balramtripathi1181@gmail.com (Balram Tripathi)

effective, are often prohibitively expensive and inaccessible for small-scale industries [5]. Consequently, there is a growing interest in developing low-cost, sustainable alternatives for wastewater treatment.

Among the various methods available for wastewater treatment, adsorption stands out as an effective, economical, and environmentally friendly approach. Adsorption is superior to other treatment methods, such as precipitation, coagulation, chemical oxidation, osmosis, and ion exchange, due to its simplicity, cost-effectiveness, and high efficiency. Biomaterials, or biosorbents, have emerged as promising alternatives for adsorption-based wastewater treatment. Biosorption involves the use of natural materials, often derived from agricultural waste, to remove pollutants. This method offers advantages such as cost efficiency, high adsorption capacity, waste minimization, and the potential for biosorbent regeneration [6–7]. A biosorbent is considered cost-effective if it is abundant in nature, readily available, and requires minimal processing before use. Hence, natural biosorbents are becoming increasingly popular as sustainable alternatives to conventional chemical and non-biodegradable adsorbents.

Activated carbon has long been recognized as one of the most effective adsorbents for wastewater treatment due to its high capacity to adsorb organic compounds. Its large surface area and the presence of oxygen-containing functional groups make it particularly effective in removing dyes, heavy metals, and other organic pollutants from aqueous solutions [8–9]. Several studies have demonstrated that carbon-rich materials can serve as efficient adsorbents for various pollutants. Activated carbon, specifically, has been observed to effectively remove micropollutants and metal ions from wastewater [10–12]. Despite its effectiveness, the relatively high cost of activated carbon limits its use, particularly in small-scale industries.

Carbon nanotubes (CNTs), discovered by Iijima in 1991, have emerged as promising alternatives to activated carbon for adsorption applications. CNTs are cylindrical nanostructures with a large surface area, unique hollow geometry, and exceptional physicochemical properties, making them highly effective as adsorbents for a wide range of pollutants [13]. They have been extensively studied for their ability to preconcentrate and immobilize contaminants from both gaseous and aqueous phases [14, 15]. The structural diversity, high selectivity, and stability of CNTs further enhance their potential as advanced adsorbents [16-18]. CNTs are classified into two types: single-walled carbon nanotubes (SWCNTs) and multi-walled carbon nanotubes (MWCNTs). While both types exhibit excellent adsorption capabilities, MWCNTs are often considered more advantageous due to their greater mechanical strength and higher surface area.

The use of CNTs for dye adsorption has gained significant attention due to their remarkable thermal, mechanical, and electrical properties. The high surface area, pore volume, and unique pore structure of CNTs contribute to their exceptional adsorption capacity. Adsorption on CNTs primarily occurs on the outer surface due to their closed ends, enabling effective chemical interactions with dye molecules [20-24]. However, one of the major limitations of CNTs is their poor solubility in aqueous and organic media, attributed to their stable structure and sp^2 bonding. The strong van der Waals forces between CNTs cause them to aggregate, making their dispersion challenging [25-28].

To overcome these limitations, functionalization of CNTs has been widely explored. Functionalization involves modifying the surface of CNTs to introduce functional groups that improve their dispersion, solubility, and interaction with adsorbates [29]. This process significantly enhances the adsorption capacity of CNTs by reducing van der Waals forces and increasing hydrophilicity. Functionalized CNTs have demonstrated remarkable potential as nanomaterials for water decontamination. Functional groups can be introduced through covalent or non-covalent bonding, either on the sidewalls or at the tips of CNTs [30]. These modifications improve the interaction between CNTs and adsorbates, facilitating efficient adsorption processes [31].

The adsorption mechanism of dyes on CNTs depends on the chemical nature of the dye molecules, particularly whether they are cationic or anionic. Various interactions, including hydrogen bonding, hydrophobic interactions, and electrostatic interactions, may occur simultaneously or individually during the adsorption process. For cationic dyes like methylene blue, CNTs provide a highly effective adsorption platform due to their negatively charged surface functional groups, which enhance electrostatic attraction [32-35]. Functionalized CNTs, therefore, offer a significant advantage in wastewater treatment applications, particularly for the removal of synthetic dyes.

In recent years, research has focused on combining CNTs with other natural materials to develop composite adsorbents with enhanced performance. Moringa oleifera leaf powder (MOLP) is one such natural material that has shown promise as a biosorbent for wastewater treatment. MOLP is abundant, inexpensive, and biodegradable, making it an ideal candidate for sustainable wastewater treatment applications. The incorporation of CNTs into MOLP can synergistically enhance its adsorption capacity, creating a composite material that leverages the advantages of both components. CNT-functionalized MOLP composites exhibit improved surface area, pore structure, and functional group availability, resulting in higher adsorption efficiencies for dyes like methylene blue [32-34].

This study aims to investigate the adsorption potential of a CNT-functionalized MOLP composite for the removal of methylene blue from aqueous solutions. By optimizing critical parameters such as pH, initial dye concentration, adsorbent dosage, temperature, and contact time, this research seeks to develop an efficient, low-cost, and environmentally friendly solution for dye-laden industrial effluents. Additionally, the study explores the synergistic effects of CNTs and MOLP, focusing on their structural, morphological, and functional characteristics. The findings of this study are expected to contribute to the development of sustainable and scalable adsorption technologies for wastewater treatment, addressing the pressing need for eco-

friendly solutions in industrial applications. The integration of CNTs with natural biosorbents like MOLP represents a promising approach to wastewater treatment. Functionalized CNTs offer superior adsorption capabilities, while MOLP provides a cost-effective and sustainable base material. The composite adsorbent developed in this study has the potential to address the challenges associated with synthetic dye removal, providing a viable alternative to conventional methods and paving the way for greener and more efficient wastewater management practices.

2. EXPERIMENTAL DETAILS

2.1. Bio-Sorbents

Moringa oleifera is a drought-resistant tree belonging to the family Moringaceae, native to the Indian subcontinent. Known as the "tree of life" in many cultures, it is extensively cultivated for its edible pods and leaves, which also have medicinal benefits. For this study, Moringa leaf powder (abbreviated as MOLP or ML) was sourced from Naveen Kaya Healthcare Ltd., Ahmedabad. The dried powder was crushed using a domestic grinder and sieved to obtain a fine, uniform consistency. The powder was stored under controlled conditions for further experimental use without undergoing any physical or chemical modifications.

The structural characteristics of the Moringa leaf powder were vital for its application as a biosorbent. Its surface properties, including porosity and the presence of functional groups, were leveraged for the adsorption of methylene blue dye. Figure 1 illustrates (a) the raw and powdered form of Moringa leaves and (b) the molecular structure of methylene blue dye.

2.2. Intercalation with CNTs

Carbon nanotubes (CNTs), synthesized using the chemical vapor deposition (CVD) method, were employed in this study. The CNTs, with a size range of 10–12 nm, were functionalized and intercalated with Moringa oleifera leaf powder (MOLP) to enhance its adsorption capacity. This intercalation process aimed to compare the adsorption efficiency of plain MOLP versus CNT-functionalized MOLP. To achieve intercalation, a fixed ratio of MOLP and CNTs was thoroughly mixed using a mechanical grinder. Subsequently, 25 mL of deionized water was added to the mixture, which was then ultrasonicated for 2 hours. Ultrasonication facilitated the uniform dispersion of CNTs within the biosorbent matrix, reducing agglomeration and enhancing the interaction between the CNTs and MOLP. The functionalized composite biosorbent was stored and used for further adsorption studies.

2.3. Methylene Blue Dye Preparation

Methylene blue (C.I. name: basic blue 9, class: thiazine, C.I. number: 52015), a cationic dye with the chemical formula $C_{16}H_8N_3Cl$ and a molecular weight of 319.9 g/mol, was sourced from Sigma Aldrich. Methylene blue was selected due to its high adsorption affinity on solid substrates and its extensive use as a dye in industries such as pulp, paper, textile, and wool manufacturing. A stock solution of methylene blue dye was prepared in distilled water, and working solutions of varying concentrations (in ppm) were prepared for equilibrium studies. These solutions were stored in covered containers to avoid photodegradation.

Fig. 1. (a) the raw and powdered form of Moringa leaves and (b) the molecular structure of methylene blue dye.

2.4. Adsorption Studies

For equilibrium adsorption studies, different concentrations of methylene blue dye solutions were prepared from the stock solution. Simultaneously, varying doses of the biosorbent (MOLP and CNT-functionalized MOLP) were prepared. Adsorption studies were conducted at room temperature under constant stirring to ensure uniform dye-biosorbent interaction. The absorbance of the dye solutions before and after the adsorption process was measured using a UV-VIS Labmann spectrophotometer at the characteristic wavelength of methylene blue. The equilibrium adsorption capacity (Q_e) of the biosorbents was calculated using the formula:

$$Qe = \frac{(Co-Ce).V}{m} \quad (1)$$

Where, C_0 is the Initial concentration of methylene blue dye (mg/L), C_e is the Equilibrium concentration of methylene blue dye (mg/L), V is the Volume of the solution (L), and m is the Mass of the adsorbent (g). This equation quantifies the amount of dye adsorbed per unit mass of the biosorbent, providing a critical parameter for evaluating the adsorption performance of the materials under investigation.

3. RESULTS AND DISCUSSION

3.1. Characterizations and properties of the materials

The surface morphology of Moringa oleifera leaf powder (MOLP) was analyzed using Scanning Electron Microscopy (SEM), revealing a heterogeneous and porous structure. The SEM images (Figure 2(a)) showed that MOLP possesses a rough surface with varying pore sizes distributed across its surface. This honeycomb-like structure, characterized by numerous micropores and cavities, provides an extensive surface area, making it highly effective for adsorption processes. The rough and porous morphology plays a critical role in enhancing the dye adsorption capacity of MOLP. The pores act as adsorption sites, allowing methylene blue molecules to bind efficiently to the surface of the biosorbent. Such morphological features make MOLP an excellent candidate for dye removal applications. The SEM image of Multi-Walled Carbon Nanotubes (MWCNTs) (Figure 2(b)) depicted the characteristic tubular and layered structures of CNTs, which were later intercalated with MOLP. The combination of MOLP and CNTs provides an augmented surface morphology with improved adsorption capabilities due to the synergistic effects of the two materials.

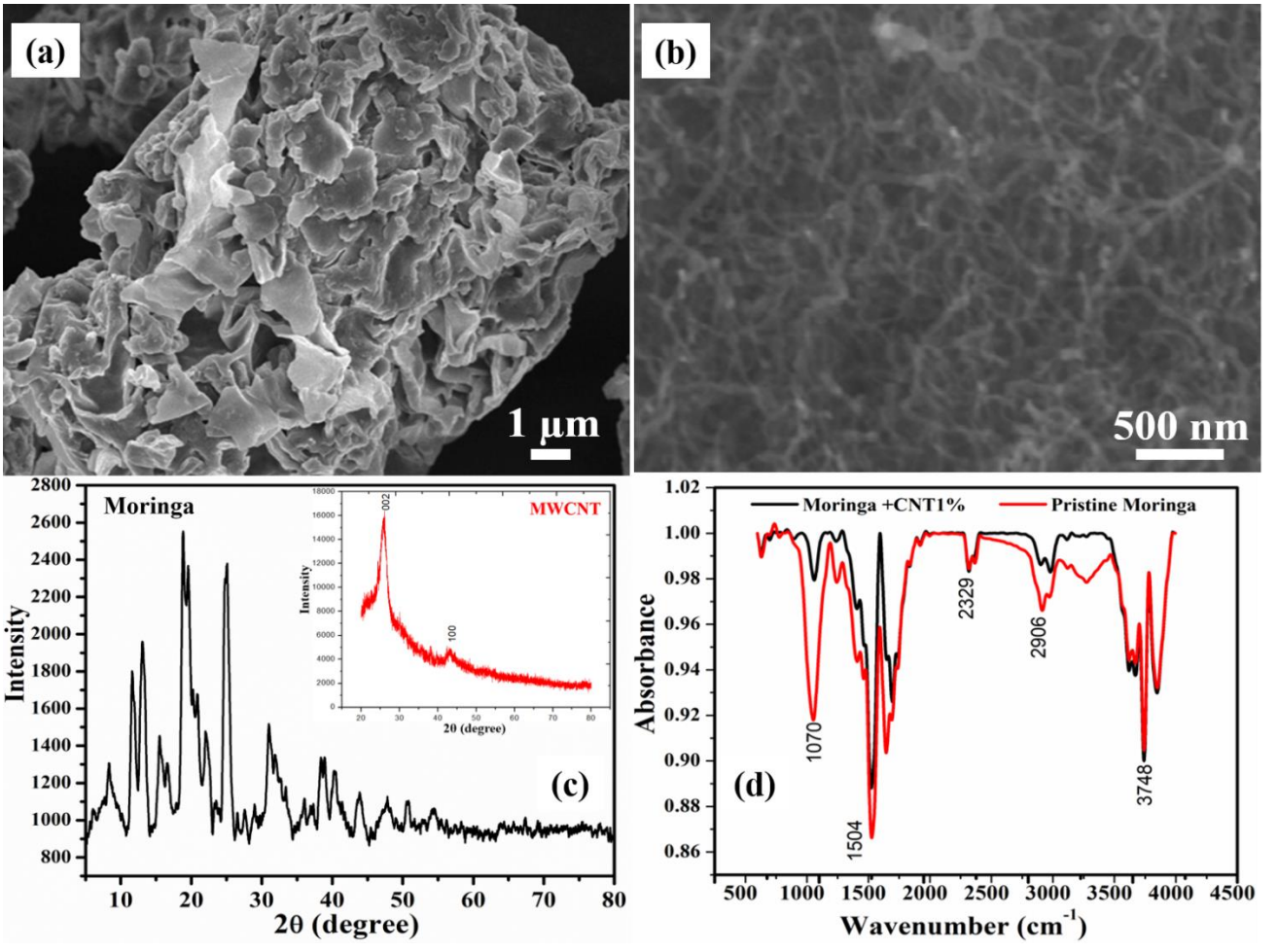

Fig. 2. SEM images of (a) pristine moringa leaves powder, (b) MWCNTs, (c) XRD pattern of moringa leaf powder and inset (c) show the XRD pattern of MWCNT, (d) FTIR spectra of pristine moringa leaf and CNT intercalated moringa leaf.

XRD analysis was conducted to investigate the crystalline structure of MOLP and CNTs. The XRD pattern of MOLP exhibited four distinct diffraction peaks at 2θ values of 15.22°, 21.81°, 22.92°, and 22.94° (Figure 2(c)). These peaks indicate that MOLP is a combination of both crystalline and amorphous phases. The broad peaks are characteristic of the amorphous components such as proteins and lipids, while the sharper peaks are associated with the crystalline cellulose and hemicellulose components of the leaf powder. The small crystallite size of the cellulose contributes to the limited sharpness of the crystalline peaks. The bioorganic substances in MOLP, including proteins, carbohydrates, and minerals, may also contribute to the unassigned peaks observed in the spectrum. This combination of amorphous and crystalline features enhances the adsorption properties of MOLP, as the amorphous regions provide flexibility while the crystalline regions contribute to structural integrity. The XRD spectrum of MWCNTs exhibited intense peaks at 26° and 44° (Figure 2(c) (inset)), corresponding to the reflections of hexagonal graphite. The peak at 26° is attributed to the graphite structure of the CNTs, indicating the high degree of crystallinity in the MWCNTs. The presence of these characteristic peaks confirms the successful synthesis of MWCNTs, which contribute additional adsorption sites and structural robustness when intercalated with MOLP.

Fourier Transform Infrared (FT-IR) spectroscopy was employed to identify functional groups in both pristine MOLP and CNT-functionalized MOLP. The FT-IR spectrum of MOLP (Figure 2(d)) exhibited distinct absorption bands, including a peak at 1062 cm^{-1} corresponding to C-OH stretching, 1577 cm^{-1} due to symmetrical C=C stretching, and 1650 cm^{-1} attributed to C=O stretching vibrations. The peaks at 2913 cm^{-1} and 3742 cm^{-1} are associated with C-H and O-H stretching, respectively [31]. In the FT-IR spectrum of raw CNTs, the O-H stretching band appeared at 3433 cm^{-1}, while peaks at 2922 cm^{-1} and 2832 cm^{-1} corresponded to asymmetric C-H stretching [32]. A pronounced dip at 1746 cm^{-1} indicated C=C stretching. When comparing the spectra of pristine MOLP and CNT-functionalized MOLP, it was observed that the number of peaks remained largely unchanged, although slight shifts in their positions occurred. The dip at 1367 cm^{-1}, attributed to C-C stretching, was more pronounced in functionalized CNTs compared to raw CNTs [33]. This enhancement suggests successful interaction between MOLP and CNTs, improving the functional properties of the biosorbent. The FT-IR results confirm the retention of key functional groups in MOLP and CNTs, which are critical for effective adsorption of methylene blue dye. The synergistic combination of MOLP and CNTs enhances both the structural and chemical properties of the biosorbent, making it highly effective for dye removal applications.

3.2. Adsorption properties

Adsorption and photocatalysis are the most commonly applied methods for reducing the amount of pollutants that enter water bodies. Among these, adsorption offers several advantages, including simplicity, cost-effectiveness, and the potential for high removal efficiency. However, one of the primary challenges in adsorption studies is the proper demonstration and interpretation of experimental data obtained from sorption processes. For many decades, researchers have relied on adsorption isotherms and kinetics to describe the adsorption process comprehensively. Commonly used models include the Langmuir and Freundlich isotherms for adsorption equilibrium studies, as well as the pseudo-first-order (PFO) and pseudo-second-order (PSO) kinetic models for understanding adsorption kinetics [36]. These models help elucidate the mechanisms and dynamics governing the adsorption process, thereby offering valuable insights into optimizing the performance of adsorbents.

3.2.1. Effect of Biosorbent Dosage

Biosorbent dosage is a critical parameter that significantly influences the adsorption capacity for a given initial concentration of dye solution. It provides insights into the efficiency and utilization of the adsorbent material. In the case of Moringa oleifera leaf powder (MOLP), it was observed that an increase in the amount of biosorbent resulted in an enhanced dye removal capacity. This phenomenon can be attributed to the increase in surface area and the availability of more adsorption sites as the biosorbent dosage increases. However, the adsorption capacity per unit mass of biosorbent decreases with increasing dosage due to the inverse proportionality between mass and adsorption capacity [37].

As depicted in Figure 3 (a-c), the adsorption capacity was found to be maximum at a biosorbent dosage of 0.001 g. Beyond this point, as the dosage of MOLP increased to 0.03 g, the adsorption capacity (qe) dropped to 0.12 mg/g. This trend can be explained by the saturation of dye molecules on the adsorbent surface at higher dosages. Additionally, at elevated dosages, the number of available MB dye molecules in solution was insufficient to occupy all the adsorption sites, resulting in a reduction in adsorption capacity per unit mass of biosorbent [38]. After achieving the optimum adsorption at a particular dosage, the adsorption process slowed down, reaching a plateau. This behavior is consistent with the principle that, at higher dosages, the aggregation of biosorbent particles may also hinder the effective diffusion of dye molecules, further reducing adsorption efficiency [39].

3.2.2. Effect of Contact Time

Contact time is another pivotal factor in determining the efficiency of the adsorption process, particularly for the removal of dye molecules such as methylene blue (MB). The relationship between contact time and adsorption efficiency

was investigated for different biosorbent dosages over a duration of 60 minutes. The results revealed a rapid adsorption phase during the initial 2 minutes, followed by a slower and more gradual phase that eventually reached equilibrium, as shown in Figure 3(d).

During the initial phase, the uptake of dye was fast due to the abundance of available adsorption sites on the biosorbent surface. However, as time progressed, the rate of adsorption slowed down and became almost constant. This is likely due to the aggregation of dye molecules on the biosorbent surface, which hindered their deeper diffusion into the adsorbent matrix [40]. At equilibrium, the adsorption sites became saturated, and the system attained a steady state. The adsorption capacity and removal percentage of MB dye were recorded at different time intervals, as summarized in Table 1. It was observed that the amount of MB adsorbed per gram of biosorbent and the removal percentage increased with time, eventually reaching a maximum at 60 minutes. This trend underscores the importance of optimizing contact time to achieve maximum dye removal efficiency.

Table 1. Adsorption capacity and removal percentage of MB dye with time.

Time (min)	Amount of MB adsorbed per gram (mg/g)	Removal Percentage (%)
5	0.1977	65.9
10	0.2043	68.1
30	0.213	73.2
40	0.2484	82.8
60	0.2787	92.9

The data indicate that rapid adsorption occurs in the initial phase, which is followed by a slower approach to equilibrium. The equilibrium adsorption capacity reflects the maximum amount of dye that can be effectively adsorbed under the given conditions [41]. These findings highlight the significance of contact time as a critical operational parameter in adsorption studies.

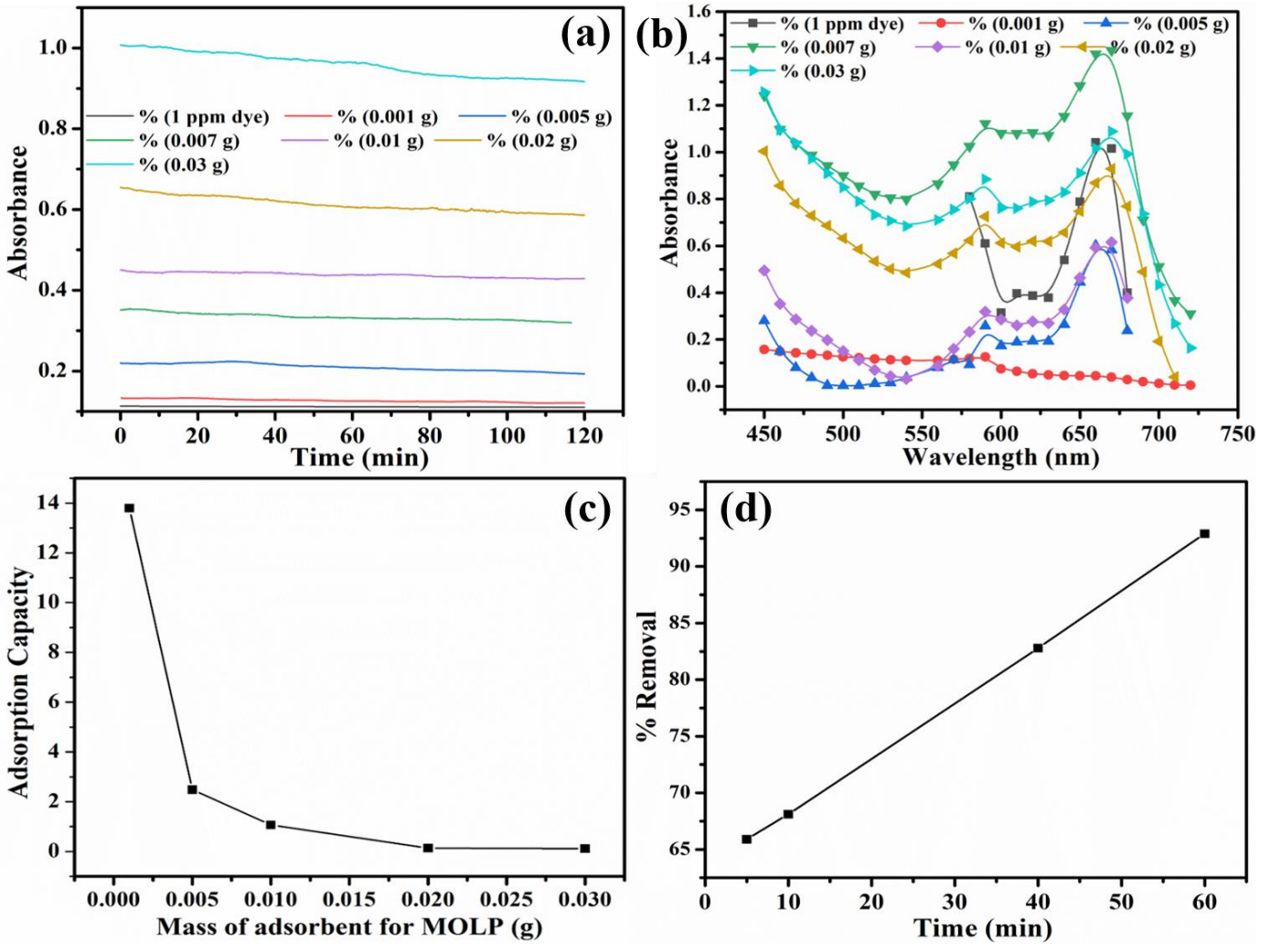

Fig. 3. (a) Absorbance with time for different doses of MOLP. (b) Absorbance vs wavelength graph for different doses of MOLP. (c) Adsorption capacity vs different doses of MOLP. (d) Removal percentage of MB dye with contact time.

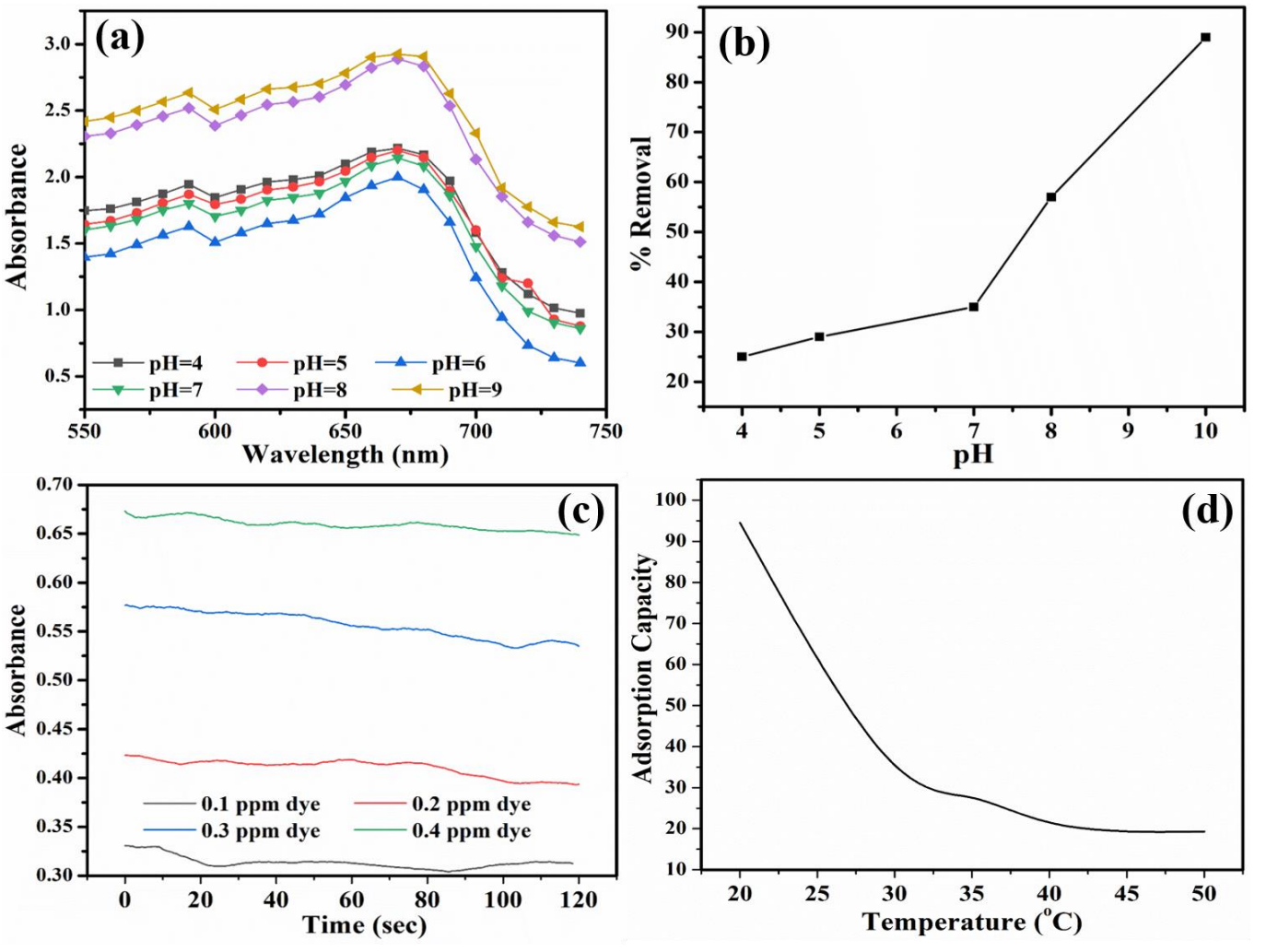

Fig. 4. (a) Absorbance vs wavelength for different pH, (b) Removal percent vs pH for MOLP (c) Removal % of MB dye vs concentration of MB (d) Variation of adsorption capacity of MOLP with temperature.

The adsorption of methylene blue dye onto Moringa oleifera leaf powder was systematically investigated, with particular attention to the effects of biosorbent dosage and contact time. The results demonstrated that an optimal biosorbent dosage and adequate contact time are essential for achieving maximum dye removal efficiency. The study also highlighted the challenges associated with high biosorbent dosages, where reduced adsorption capacity per unit mass and particle aggregation can hinder the process. Similarly, the importance of optimizing contact time was emphasized, as prolonged durations lead to equilibrium saturation. The use of adsorption isotherms and kinetic models provided a deeper understanding of the mechanisms governing the adsorption process.

3.2.3. Effect of pH

pH plays a crucial role in determining the efficiency of the adsorption process due to its impact on the acid-base properties of functional groups present on the biosorbent surface. The pH was adjusted using 1M NaOH and 1M HCl, as it significantly influences the electrostatic interactions between the ionized dye molecules and the biosorbent surface. The adsorption of methylene blue (MB) dye was found to be lower at lower pH levels, primarily because the increased concentration of H^+ ions competes with the cationic dye molecules for binding sites on the adsorbent. However, as the pH increased, the number of negatively charged adsorption sites on the biosorbent surface also increased, thereby enhancing the adsorption of cationic MB dye (Figure 4).

At a pH of 4, the removal percentage of MB dye was observed to be 25%, which increased significantly to 80% as the pH was raised to 10. This trend can be attributed to the enhanced availability of negatively charged sites at higher pH, which facilitates stronger electrostatic interactions with the cationic dye molecules. This observation aligns with previous studies that reported improved adsorption of cationic dyes under alkaline conditions [42, 43].

3.2.4. Effect of Initial Dye Concentration

The initial concentration of the dye is another critical parameter influencing the adsorption process. As shown in Figure 4(d), the removal efficiency of MB dye was initially high (approximately 90%) when the dye concentration was 0.1 ppm. However, as the concentration increased to 0.5 ppm, the removal percentage decreased to 50%. This decline can be attributed to the saturation of available adsorption sites on the biosorbent surface at higher dye concentrations, resulting in increased competition among dye molecules for the limited binding sites.

At lower dye concentrations, the number of vacant adsorption sites on the biosorbent surface is significantly higher than the number of dye molecules, leading to efficient adsorption. However, as the concentration of dye increases, the ratio of dye molecules to available binding sites also increases, resulting in a decrease in the overall removal efficiency. This behavior has been widely reported in the literature [44, 45]. Table 2 shows the % removal of dye at different temperature.

Table 2. Percentage Removal of Dye at Different Temperatures.

Temperature (ºC)	Amount of MB adsorbed per gm
20	**94.5**
30	**27.1**
35	**29.8**
40	**19.0**
50	**19.3**

3.2.5. Effect of Temperature

Temperature has a profound impact on the adsorption process, as it influences both the structural properties of the biosorbent and the diffusion rate of dye molecules. The adsorption capacity of the biosorbent decreased with increasing temperature, as shown in Figure 4(d) and Table 2. At 20°C, the removal efficiency of MB dye was 94.5%, which decreased to 19.3% at 50°C. Two primary factors contribute to this trend. First, an increase in temperature reduces the viscosity of the dye solution, which facilitates faster diffusion of dye molecules onto the adsorbent surface. However, it also leads to an increase in desorption rates, which reduces the net adsorption capacity [46]. Second, higher temperatures can deactivate the functional groups on the biosorbent surface or destroy active sites, thereby reducing the overall adsorption efficiency [43].

3.2.6. Effect of Functionalization

While carbon nanotubes (CNTs) are known for their high adsorption potential, their practical application in water treatment is often limited due to their poor solubility in aqueous media. This issue arises from their stable sp^2 bonding and strong van der Waals forces, which cause CNTs to aggregate, making them difficult to disperse uniformly [47]. To address this, the current study utilized an ultrasonicator to intercalate Moringa leaves powder (MOLP) with CNTs and evaluated their efficiency as adsorbents.

As shown in Figure 5, the adsorption capacity of pristine MOLP was compared with that of functionalized CNTs. It was observed that the addition of 1% CNT improved the adsorption efficiency significantly, outperforming pristine MOLP. However, further increasing the CNT concentration to 3% and 5% led to a decline in removal efficiency. This reduction may be attributed to the blockage of adsorption sites due to excessive CNT loading, which limits the availability of active sites for dye adsorption. The adsorption process for both pristine MOLP and 1% CNT-functionalized MOLP was monitored over a 60 minutes period. Rapid adsorption was observed within the initial 10 minutes for the 1% CNT sample, followed by a steady-state equilibrium phase. This suggests that while the rate of adsorption is high initially, it eventually stabilizes as the adsorption sites become saturated [47].

Additionally, Figure 6 highlights the effect of temperature on the adsorption efficiency of CNT-functionalized MOLP. At lower temperatures (20°C), 1% CNT exhibited the highest adsorption capacity compared to 3% and 5% CNT, as well as pristine MOLP. However, with increasing temperature, the adsorption efficiency declined, which can be attributed to desorption and the possible deactivation of functional groups on the biosorbent surface. This finding aligns with previous reports that functionalized CNTs improve adsorption efficiency at moderate temperatures but may suffer from reduced performance at higher temperatures [46, 47].

The adsorption of methylene blue dye using MOLP and functionalized CNTs was systematically studied to understand the effects of various operational parameters, including pH, initial dye concentration, temperature, and functionalization. It was found that pH plays a critical role in modulating the adsorption process by influencing the electrostatic interactions between dye molecules and the adsorbent surface. Similarly, the initial dye concentration determines the availability of binding sites, with higher concentrations leading to reduced adsorption efficiency. Temperature, on the other hand, affects both the diffusion of dye molecules and the stability of biosorbent functional groups, with higher temperatures resulting in decreased adsorption efficiency.

Functionalization of MOLP with CNTs emerged as a promising strategy to enhance adsorption performance. The study revealed that 1% CNT-functionalized MOLP exhibited superior adsorption capacity compared to pristine MOLP, highlighting the potential of functionalized adsorbents for water treatment applications. However, the efficiency declined with excessive CNT loading, emphasizing the need for optimal functionalization to achieve maximum performance. The findings of this study contribute to the growing body of knowledge on the use of biosorbents and

functionalized materials for environmental remediation. Future work should focus on scaling up the process for real-world applications and exploring the potential of other functionalization techniques to further enhance adsorption efficiency.

4. CONCLUSION

This research emphasizes the potential of CNT-intercalated Moringa oleifera leaf powder (MOLP) as an effective and sustainable adsorbent for the removal of methylene blue (MB) dye from aqueous solutions. By systematically optimizing critical parameters, including pH, initial dye concentration, adsorbent dosage, temperature, and contact time, the study has established an efficient protocol for maximizing adsorption capacity. The synergistic role of CNTs in enhancing the adsorption efficiency of MOLP was demonstrated through detailed morphological and spectroscopic analyses. SEM analysis revealed a highly porous structure in CNT-functionalized MOLP, which facilitates enhanced dye entrapment compared to pristine MOLP. The presence of functional groups, such as carboxylic, carbonyl, and phenolic groups, was confirmed through FT-IR spectroscopy, and these groups play a pivotal role in forming hydrogen bonds and electrostatic interactions with MB dye molecules. The incorporation of CNTs further improved the material's adsorption capabilities due to their high surface area, superior pore structure, and ability to be functionalized for improved dispersion and solubility. This study demonstrates that CNT-functionalized MOLP is a viable alternative to expensive commercial adsorbents like activated carbon. The results highlight its potential application in industries where dye-laden effluents pose severe environmental risks. Additionally, the biosorbent's biodegradable and cost-effective nature makes it an attractive solution for small-scale industries that cannot afford conventional wastewater treatment methods. Future work may explore the reusability of the bio-composite and its efficiency for removing other pollutants, thereby broadening its applicability in environmental remediation.

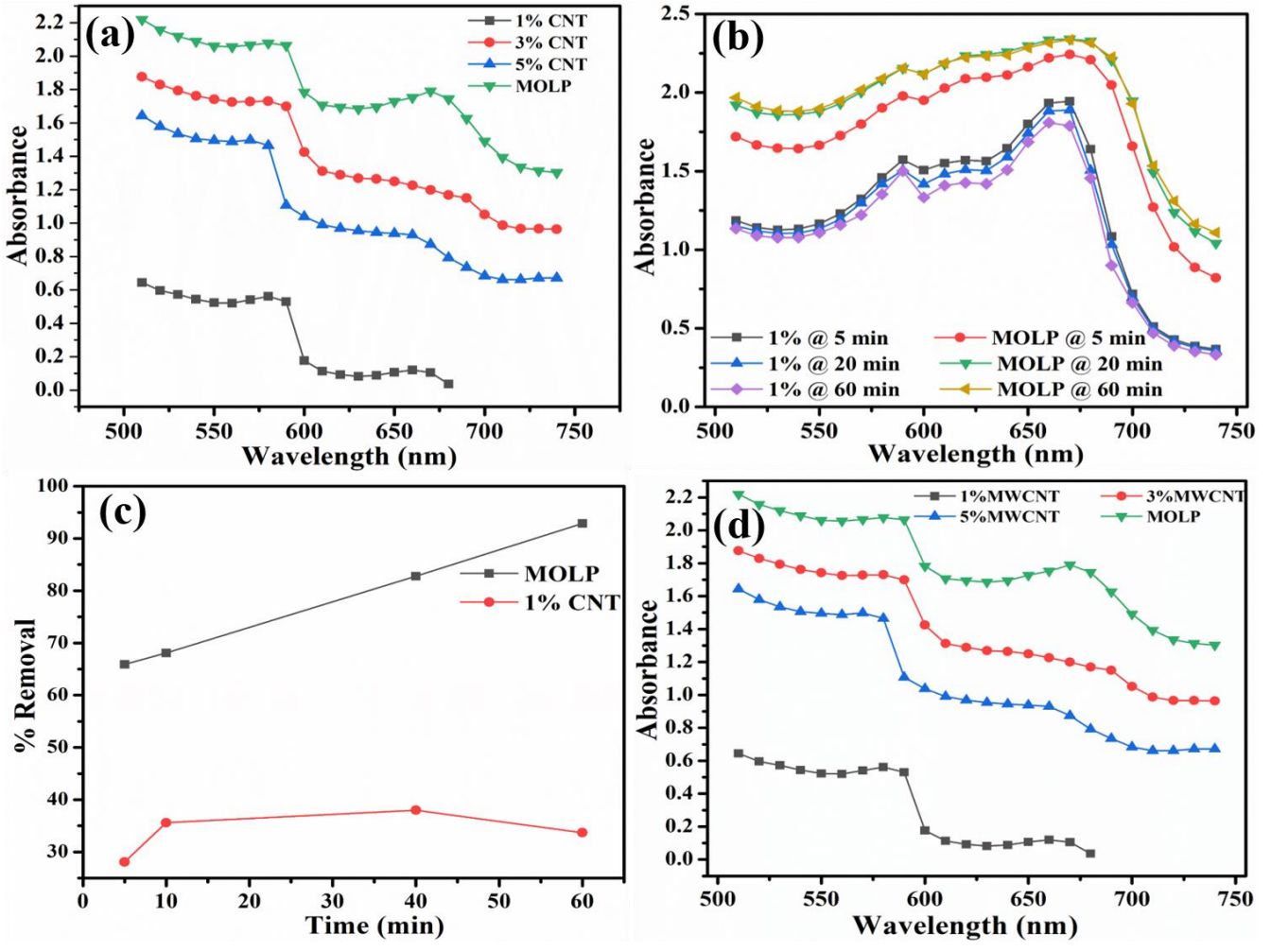

Fig. 5. (a) Absorbance vs. wavelength graph for pristine MOLP and functionalized CNT; (b) Comparison of absorbance between 1% CNT and pristine MOLP over time; (c) Comparison of dye removal percentage for 1% CNT and pristine MOLP over time; (d) Absorbance vs. wavelength spectra for pristine MOLP and functionalized CNT.

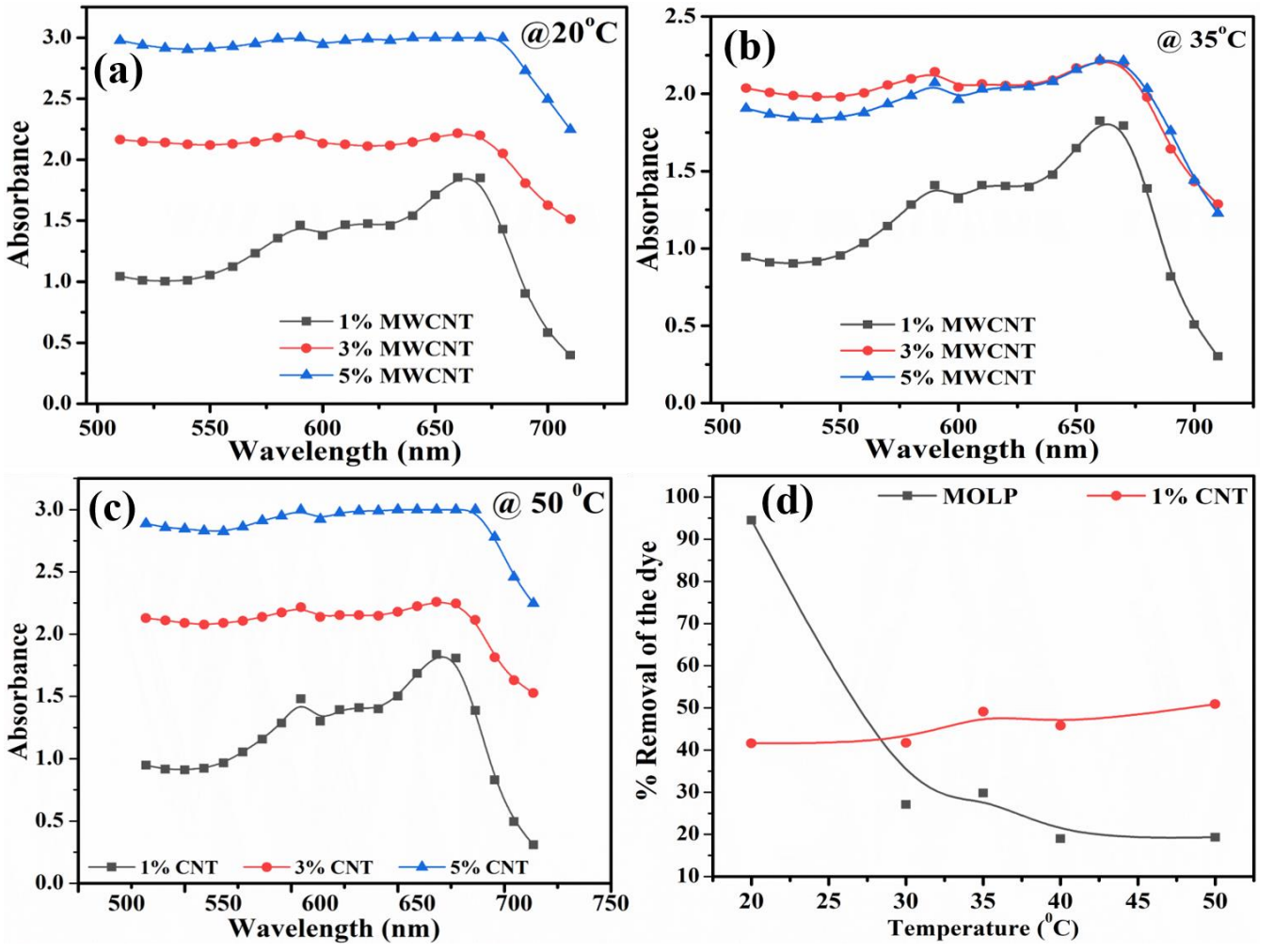

Fig. 6. (a) Absorbance of 1%, 3%, and 5% CNT at 20°C; (b) Absorbance of 1%, 3%, and 5% CNT at 35°C; (c) Absorbance of 1%, 3%, and 5% CNT at 50°C; (d) Comparison of dye removal percentage for pristine MOLP and 1% CNT at different temperatures.

DECLARATIONS

Ethical Approval

We affirm that this manuscript is an original work, has not been previously published, and is not currently under consideration for publication in any other journal or conference proceedings. All authors have reviewed and approved the manuscript, and the order of authorship has been mutually agreed upon.

Funding

Not applicable

Availability of data and material

All of the data obtained or analyzed during this study is included in the report that was submitted.

Conflicts of Interest

The authors declare that they have no financial or personal interests that could have influenced the research and findings presented in this paper. The authors alone are responsible for the content and writing of this article.

Authors' contributions

All authors contributed equally in the preparation of this manuscript.

ACKNOWLEDGEMENTS

Authors are thankful to DST Govt. of India for financial assistance under DST-FIST (SR/FST/College/2020/1003) Scheme & SAIF Manipal University Jaipur, Jaipur, India for providing SEM facility.

REFERENCES

[1] Ayed, L., Mahdhi, A., Cheref, A. and Bakhrouf, A., **2011.** Decolorization and degradation of azo dye Methyl Red by an isolated Sphingomonas paucimobilis: biotoxicity and metabolites characterization. *Desalination*, *274*(1-3), pp.272-277.

[2] Vinoda, B.M., Vinuth, M., Bodke, Y.D. and Manjanna, J., **2015.** Photocatalytic degradation of toxic methyl red dye using silica nanoparticles synthesized from rice husk ash. *Journal of Environmental & Analytical Toxicology. 5*(6), p.1000336.

[3] Ahmad, M.A., Ahmad, N. and Bello, O.S., **2015.** Modified durian seed as adsorbent for the removal of methyl red dye from aqueous solutions. *Applied Water Science*, *5*, pp.407-423.

[4] Gong, J.L., Wang, B., Zeng, G.M., Yang, C.P., Niu, C.G., Niu, Q.Y., Zhou, W.J. and Liang, Y., **2009.** Removal of cationic dyes from aqueous solution using magnetic multi-wall carbon nanotube nanocomposite as adsorbent. *Journal of Hazardous Materials*, *164*(2-3), pp.1517-1522.

[5] Groeneveld, I., Kanelli, M., Ariese, F. and van Bommel, M.R., **2023**. Parameters that affect the photodegradation of dyes and pigments in solution and on substrate–An overview. *Dyes and Pigments*, *210*, p.110999.

[6] Joshua, R. and Vasu, V., **2013.** Characteristics of stored rain water and its treatment technology using Moringa seeds. *International Journal of Life Sciences Biotechnology and Pharma Research*, *2*(1), p.19.

[7] Araujo, C.S., Alves, V.N., Rezende, H.C., Almeida, I.L., de Assuncao, R.M., Tarley, C.R., Segatelli, M.G. and Coelho, N.M.M., **201**0. Characterization and use of Moringa oleifera seeds as biosorbent for removing metal ions from aqueous effluents. *Water Science and Technology*, *62*(9), pp.2198-2203.

[8] Altmann, J., Rehfeld, D., Träder, K., Sperlich, A. and Jekel, M., **2016.** Combination of granular activated carbon adsorption and deep-bed filtration as a single advanced wastewater treatment step for organic micropollutant and phosphorus removal. *Water research*, *92*, pp.131-139.

[9] Guillossou, R., Le Roux, J., Mailler, R., Vulliet, E., Morlay, C., Nauleau, F., Gasperi, J. and Rocher, V., **2019.** Organic micropollutants in a large wastewater treatment plant: what are the benefits of an advanced treatment by activated carbon adsorption in comparison to conventional treatment? *Chemosphere*, *218*, pp.1050-1060.

[10] Xiong, C., Jia, Q., Chen, X., Wang, G. and Yao, C., **2013.** Optimization of polyacrylonitrile-2-aminothiazole resin synthesis, characterization, and its adsorption performance and mechanism for removal of Hg (II) from aqueous solutions. *Industrial & Engineering Chemistry Research*, *52*(14), pp.4978-4986.

[11] Huang, J., Cao, Y., Shao, Q., Peng, X. and Guo, Z., **2017.** Magnetic nanocarbon adsorbents with enhanced hexavalent chromium removal: morphology dependence of fibrillar vs particulate structures. *Industrial & Engineering Chemistry Research*, *56*(38), pp.10689-10701.

[12] Queiroz, L.S., de Souza, L.K., Thomaz, K.T.C., Lima, E.T.L., da Rocha Filho, G.N., do Nascimento, L.A.S., de Oliveira Pires, L.H., Faial, K.D.C.F. and da Costa, C.E., **2020.** Activated carbon obtained from amazonian biomass tailings (acai seed): Modification, characterization, and use for removal of metal ions from water. *Journal of Environmental Management*, *270*, p.110868.

[13] Wumair, T., Dou, J., Zhang, L., Chen, M. and Kang, X., **2013.** Synthesis of carbon microtubules core structure LiFePO 4 via a template-assisted method. *Ionics*, *19*, pp.1855-1860.

[14] Baughman, R.H., Zakhidov, A.A. and De Heer, W.A., **2002.** Carbon nanotubes--the route toward applications. *Science*, *297*(5582), pp.787-792.

[15] Ren, X., Chen, C., Nagatsu, M. and Wang, X., **2011.** Carbon nanotubes as adsorbents in environmental pollution management: a review. *Chemical Engineering Journal*, *170*(2-3), pp.395-410.

[16] Rajabi, M., Mahanpoor, K. and Moradi, O., **2017.** Removal of dye molecules from aqueous solution by carbon nanotubes and carbon nanotube functional groups: critical review. *RSC Advances*, *7*(74), pp.47083-47090.

[17] Bankole, M.T., Abdulkareem, A.S., Mohammed, I.A., Ochigbo, S.S., Tijani, J.O., Abubakre, O.K. and Roos, W.D., **2019.** Selected heavy metals removal from electroplating wastewater by purified and polyhydroxylbutyrate functionalized carbon nanotubes adsorbents. *Scientific Reports*, *9*(1), p.4475.

[18] Ruoff, R.S. and Lorents, D.C., **1995.** Mechanical and thermal properties of carbon nanotubes. *Carbon*, *33*(7), pp.925-930.

[19] Moreira, L., Fulchiron, R., Seytre, G., Dubois, P. and Cassagnau, P., **2010.** Aggregation of carbon nanotubes in semidilute suspension. *Macromolecules*, *43*(3), pp.1467-1472.

[20]Hayati, B., Maleki, A., Najafi, F., Daraei, H., Gharibi, F. and McKay, G., **2017.** Super high removal capacities of heavy metals (Pb^{2+} and Cu^{2+}) using CNT dendrimer. *Journal of Hazardous Materials*, *336*, pp.146-157.

[21]Huang, T.S., Tzeng, Y., Liu, Y.K., Chen, Y.C., Walker, K.R., Guntupalli, R. and Liu, C., **2004.** Immobilization of antibodies and bacterial binding on nanodiamond and carbon nanotubes for biosensor applications. *Diamond and Related Materials*, *13*(4-8), pp.1098-1102.

[22]Barman, B.K. and Nanda, K.K., **2016.** Prussian blue as a single precursor for synthesis of Fe/Fe_3C encapsulated N-doped graphitic nanostructures as bi-functional catalysts. *Green Chemistry*, *18*(2), pp.427-432.

[23]Huang, X., Liang, K.H., Liu, Q., Qiu, J., Wang, J. and Zhu, H., **2020.** Superfine grinding affects physicochemical, thermal and structural properties of Moringa Oleifera leaf powders. *Industrial Crops and Products*, *151*, p.112472.

[24]Gopalakrishnan, L., Doriya, K. and Kumar, D.S., **2016.** Moringa oleifera: A review on nutritive importance and its medicinal application. *Food Science and Human Wellness*, *5*(2), pp.49-56.

[25]Cao, A., Xu, C., Liang, J., Wu, D. and Wei, B., **2001.** X-ray diffraction characterization on the alignment degree of carbon nanotubes. *Chemical Physics Letters*, *344*(1-2), pp.13-17.

[26]Abebe, B., Murthy, H.A. and Amare, E., **2018.** Summary on adsorption and photocatalysis for pollutant remediation: mini review. *Journal of Encapsulation and Adsorption Sciences*, *8*(4), pp.225-255.

[27]Bello, O.S., Adegoke, K.A. and Akinyunni, O.O., **2017.** Preparation and characterization of a novel adsorbent from Moringa oleifera leaf. *Applied Water Science*, *7*, pp.1295-1305.

[28]Do, T.H., Dung, N.Q., Chu, M.N., Van Kiet, D., Ngan, T.T.K. and Van Tan, L., **2021.** Study on methylene blue adsorption of activated carbon made from Moringa oleifera leaf. *Materials Today: Proceedings*, *38*, pp.3405-3413.

[29]Kuang, Y., Zhang, X. and Zhou, S., **2020.** Adsorption of methylene blue in water onto activated carbon by surfactant modification. *Water*, *12*(2), p.587.

[30]Mordhiya, B., Daga, K., Chandra, S. and Aggarwal, S**., 2012.** Adsorptive treatment of Methylene blue dye from aqueous solution using Moringa oleifera as an adsorbent. *Nature, Environment and Pollution Technology*, *11*(1), pp.113-116.

[31]Sudrajat, H., Susanti, A., Putri, D.K.Y. and Hartuti, S., **2021.** Mechanistic insights into the adsorption of methylene blue by particulate durian peel waste in water. *Water Science and Technology*, *84*(7), pp.1774-1792.

[32]Saleem, M., Pirzada, T. and Qadeer, R., **2007.** Sorption of acid violet 17 and direct red 80 dyes on cotton fiber from aqueous solutions. *Colloids and Surfaces A: Physicochemical and Engineering Aspects*, *292*(2-3), pp.246-250.

[33]Sarı, A. and Tuzen, M., **2008.** Biosorption of cadmium (II) from aqueous solution by red algae (Ceramium virgatum): equilibrium, kinetic and thermodynamic studies. *Journal of Hazardous Materials*, *157*(2-3), pp.448-454.

[34]Moreira, L., Fulchiron, R., Seytre, G., Dubois, P. and Cassagnau, P., **2010.** Aggregation of carbon nanotubes in semidilute suspension. *Macromolecules*, *43*(3), pp.1467-1472.

[35]Chen, Q., Saltiel, C., Manickavasagam, S., Schadler, L.S., Siegel, R.W. and Yang, H., **2004.** Aggregation behavior of single-walled carbon nanotubes in dilute aqueous suspension. *Journal of Colloid and Interface Science*, *280*(1), pp.91-97.

[36]Ali, H., Khan, E. and Sajad, M.A**., 2013.** Phytoremediation of heavy metals—concepts and applications. *Chemosphere*, *91*(7), pp.869-881.

[37]Faezah, J.N., Yusliza, M.Y., Azlina, Y.N., Saputra, J. and Zulkifli, W.K.W., **2022.** Developing a conceptual model to implement the employee ecological behavior in organisations. *Journal of Environmental Management & Tourism*, *13*(3), pp.746-755.

[38]Yadav, S., Yadav, A., Bagotia, N., Sharma, A.K. and Kumar, S., **2021.** Adsorptive potential of modified plant-based adsorbents for sequestration of dyes and heavy metals from wastewater-A review. *Journal of Water Process Engineering*, *42*, p.102148.

[39]Sah, M.K., Edbey, K., EL-Hashani, A., Almshety, S., Mauro, L., Alomar, T.S., AlMasoud, N. and Bhattarai, A., **2022.** Exploring the biosorption of methylene blue dye onto agricultural products: A critical review. *Separations*, *9*(9), p.256.

[40]Saba, B., Christy, A.D. and Jabeen, M., **2016.** Kinetic and enzymatic decolorization of industrial dyes utilizing plant-based biosorbents: a review. *Environmental Engineering Science*, *33*(9), pp.601-614.

[41]Wu, H.Y., Chen, S.S., Liao, W., Wang, W., Jang, M.F., Chen, W.H., Ahamad, T., Alshehri, S.M., Hou, C.H., Lin, K.S. and Charinpanitkul, T., **2020.** Assessment of

agricultural waste-derived activated carbon in multiple applications. *Environmental Research*, *191*, p.110176.

[42] Auta, M. and Hameed, B.H., **2014.** Chitosan–clay composite as highly effective and low-cost adsorbent for batch and fixed-bed adsorption of methylene blue. *Chemical Engineering Journal*, *237*, pp.352-361.

[43] Foo, K.Y. and Hameed, B.H., **2010.** Insights into the modeling of adsorption isotherm systems. *Chemical Engineering Journal*, *156*(1), pp.2-10.

[44] Ho, Y.S. and McKay, G., **1999.** Pseudo-second order model for sorption processes. *Process Biochemistry*, *34*(5), pp.451-465.

[45] Rafatullah, M., Sulaiman, O., Hashim, R. and Ahmad, A., **2010.** Adsorption of methylene blue on low-cost adsorbents: a review. *Journal of Hazardous Materials*, *177*(1-3), pp.70-80.

[46] Vijayaraghavan, K., Jegan, J., Palanivelu, K. and Velan, M., **2005.** Biosorption of copper, cobalt and nickel by marine green alga Ulva reticulata in a packed column. *Chemosphere*, *60*(3), pp.419-426.

[47] Tachikawa, Y., Ito, M., Irita, M., Harada, T. and Umemura, K., **2024.** Near-Infrared Photoluminescence Responses of Single-Walled Carbon Nanotubes Induced by Biomolecules Detected on a Microbead Surface. *ACS Omega*, *9*(44), pp.44734-44740.